JASMAC
Conference of the Japan Society of Microgravity Application

OR3-3

濡れ性を考慮したマランゴニ対流の気液二相流数値解析に向けた手法検討

Examination of a method for gas-liquid two-phase numerical analysis of Marangoni convection considering wettability

○牧 晴也[1], 田川 俊夫[1]
○Seiya MAKI[1], Toshio TAGAWA[1]
1 東京都立大学大学院システムデザイン研究科 航空宇宙システム工学域, Department of Aeronautics and Astronautics, Tokyo Metropolitan University

1. Introduction

It is widely known that Marangoni convection, which is one of the thermo-fluid phenomena caused by the temperature dependency of surface tension, has a great influence on the quality of the crystals produced by the Floating Zone method, which is one of the methods for manufacturing silicon single crystals. If the mechanism of Marangoni convection can be elucidated and successfully controlled, it is highly useful for engineering purposes, such as improving crystal purity.

However, the conventional numerical methods for gas-liquid two-phase flows, such as the Volume of Fluid (VOF) method, the Level Set method, and the Coupled Level Set /Volume of Fluid (CLSVOF) method, are said to have the following two problems. The interface width diffuses and becomes non-uniform during the calculation, and velocity oscillations occur due to switching the treatment near the interface region. Therefore, in this paper, we examine a method suitable for fluid phenomena where surface tension is dominant.

Based on this background, in the present study, the Conservative Phase Field method [1)] was introduced as a method to calculate the advection of the interface function while maintaining the interface width, without including the switching of treatment near the interface region. By coupling with the Level Set method, we aim to improve the accuracy of interface behavior prediction. In this study, to expand the computational scope of the method, we attempt to apply the method to (A) wettability on solid walls and (B) Marangoni convection when temperature dependency is considered and investigate its usefulness by calculating benchmark problems.

2. Numerical method

2.1 Governing equation

The governing equations used in this study are as follows.

＜Continuity equation for incompressible flow＞

$$\vec{\nabla} \cdot \vec{u} = 0 \tag{1}$$

＜Navier Stokes equation＞

$$\frac{\partial \vec{u}}{\partial t} + (\vec{u} \cdot \vec{\nabla})\vec{u} = -\frac{1}{\rho}\vec{\nabla}p + \frac{1}{\rho}\vec{\nabla} \cdot (2\mu \boldsymbol{D}) + \frac{1}{\rho}\vec{f}_{sf} \tag{2}$$

＜Strain rate tensor＞

$$\boldsymbol{D} = \frac{1}{2}\begin{bmatrix} 2\dfrac{\partial u}{\partial x} & \dfrac{\partial u}{\partial y} + \dfrac{\partial v}{\partial x} \\ \dfrac{\partial v}{\partial x} + \dfrac{\partial u}{\partial y} & 2\dfrac{\partial v}{\partial y} \end{bmatrix} \tag{3}$$

＜Energy equation＞

$$\frac{\partial T}{\partial t} + (\vec{u} \cdot \vec{\nabla})T = \frac{1}{\rho C_p}\vec{\nabla} \cdot (k\,\vec{\nabla}\,T) \tag{4}$$

＜Advection equation for interface function＞

$$\frac{\partial \phi}{\partial t} + (\vec{u} \cdot \vec{\nabla})\phi = M\left[\nabla^2\phi - \vec{\nabla} \cdot \left[\frac{4\phi(1-\phi)}{\epsilon}\frac{\nabla\phi}{|\nabla\phi|}\right]\right] + \beta(t)\sqrt{\phi^2(1-\phi^2)} \tag{5}$$

＜Treatment of mass conservation＞

$$\beta(t) = \frac{m_0 - m}{\sum_{i=1}^{nx}\sum_{j=1}^{ny}\sqrt{\phi^2(1-\phi^2)}} \tag{6}$$

In this study, incompressible Newtonian fluid is assumed, and phase change is not considered. The Red & Black HSMAC method is used for the pressure-modified solution to satisfy the incompressible condition. The governing equations, which are nondimensionalized from Eqs. (1)-(5), are spatially discretized on an equally spaced Cartesian grid using the finite difference method, and the Euler explicit method is used to discretize the time term. The energy equation is not solved in the calculation assuming an isothermal field.

The $\vec{f}_{sf}$ in Eq. (2) is the surface tension term, and the treatment of this term is discussed in Section 2.3.

M in Eq. (5) is the interfacial mobility, which takes the value corresponding to the maximum velocity at the interfacial region. ϵ is the interfacial width, which is set to about three grids in this study. ϕ is the interfacial discriminant function, called the order parameter used in the Conservative Phase Field method, where $\phi = 1$ represents the liquid phase, and $\phi = 0$ represents the gas phase, and the intermediate $\phi = 0.5$ represents the gas-liquid interface position.

In the Conservative Phase Field method, the Conservative Allen-Cahn equation expressed in Eq. (5) is used as the advection equation of the interface function, so that the order parameter ϕ representing the gas-liquid interface is kept in the form of an equilibrium solution expressed by the hyperbolic tangent function of the distance from the gas-liquid interface, and the interface width is kept constant in the computational domain.

In addition, $\beta(t)\sqrt{\phi^2(1-\phi^2)}$ in Eq. (5) is a mass correction term[2] to strictly satisfy the mass conservation, and $\beta(t)$ is expressed by Eq.(6). In Eq. (6), m_0 is the initial liquid phase volume, and m is the liquid phase volume at the time of calculation.

The values of ρ, μ, C_p, and k in each equation are the density, viscosity, isobaric specific heat capacity, and thermal conductivity, respectively. In the actual calculation, the order parameter ϕ is used to switch these values to those in each phase to express these values that vary with phase.

2.2 Coupling with the Level Set method

In this study, we use the inverse functional equation (7) to calculate the signed distance function ψ corresponding to the ordered parameter after the advection calculation. Then, the reinitialization operation used in the Level Set method is performed on ψ to fully recover its properties as a distance function for the region near the interface.

The signed distance function ψ obtained by these operations is used to calculate the normal vectors in the governing equations and the interface curvature, aiming to obtain the interface behavior with high accuracy. In addition, it is possible to use various Continuum Surface Force (CSF) models that have been devised for Level Set functions.

$$\psi = \begin{cases} 1.5\epsilon & (\phi > 1.0 - 10^{-3}) \\ \frac{\epsilon}{4}\log\left(\frac{\phi - 1}{\phi}\right) & (10^{-3} \le \phi \le 1.0 - 10^{-3}) \\ -1.5\epsilon & (\phi < 10^{-3}) \end{cases} \tag{7}$$

2.3 Treatment of the surface tension term

The surface tension term $\vec{f}_{sf}$ in the isothermal field is expressed by equation (8) using the interfacial curvature κ and the surface tension coefficient σ_0.

$$\vec{f}_{sf} = \frac{1}{\rho}\sigma_0 \kappa \vec{\nabla} H_\alpha^{sc}(\psi) \tag{8}$$

When temperature dependency is considered, the surface tension term $\vec{f}_{sf}$ is expressed in Eq. (9) using the temperature coefficient of surface tension σ_T Here, $\vec{\nabla}_s$ in Eq. (9) represents the differential operator tangential to the interface.

$$\vec{f}_{sf} = \frac{1}{\rho}\left(\sigma_0 \kappa \vec{\nabla} H_\alpha^{sc}(\psi) - \sigma_\theta \kappa \vec{\nabla} H_\alpha^{sc}(\psi)(T - T_0) - \sigma_T \frac{dH_\alpha^{sc}(\psi)}{d\psi} \vec{\nabla}_s T\right) \tag{9}$$

In this study, the Density-Scaled Balanced CSF model proposed by Yokoi et al [3]. is used to discretize the surface tension term, and $H_\alpha^{sc}(\psi)$ in the equation is the density-scaled approximate Heaviside function. $H_\alpha^{sc}(\psi)$ is expressed in equation (10) using the signed distance function ψ.

$$H_\alpha^{sc}(\psi) = \begin{cases} 0 & \text{if } \psi < -\epsilon \\ \frac{1}{2}\left[\frac{1}{2} + \frac{\psi}{\epsilon} + \frac{\psi^2}{2\epsilon^2} - \frac{1}{4\pi^2}\left(\cos\left(\frac{2\pi\psi}{\epsilon}\right) - 1\right) + \frac{\epsilon + \psi}{\epsilon\pi}\sin\left(\frac{\pi\psi}{\epsilon}\right)\right] & \text{if } |\psi| \le \epsilon \\ 1 & \text{if } \psi > \epsilon \end{cases} \tag{10}$$

2.4 Wettability boundary condition

In this study, following the example proposed by Liu et al [4]. and verified by Fakhari et al [5]. using the lattice Boltzmann method, the boundary conditions for the ordered parameter on the wall are given by Equation (11) to simulate the wettability on a solid wall:

$$\vec{n}_w \cdot \vec{\nabla}\phi = -\frac{4}{\epsilon}\cos\theta_{th}\phi_w(1 - \phi_w) \tag{11}$$

where, $\vec{n}_w$ is the normal vector of the wall, ϕ_w is the order parameter on the wall, and θ_{th} is the set contact angle.

3. Validation

3.1 (A) Droplet deformation due to wettability on a flat solid wall

To validate the wettability boundary condition, the droplet deformation due to wettability on a flat solid wall is simulated. In this problem, a semicircular droplet is placed on the wall as the initial condition, and the deformation of the droplet to satisfy the set contact angle is simulated. The height and horizontal length of the droplet at a steady state are compared with the analytical solution.

3.1.1 Computational model

The computational model used for the validation in this section is shown in **Fig. 1**. The physical properties of the working fluid used in the analysis are shown in **Table 1**. The definitions of the droplet radius R_0 in the initial shape, the droplet radius R_0, the horizontal length L of the droplet on the wall, and the maximum vertical length e from the wall in the

final shape, which are used for comparison with the analytical solution, are illustrated in **Fig. 2**.

Table 1 Physical parameters of the fluid

Symbol	Name	Fluid 1	Fluid 2	Unit
ρ	Density	1000	1.0	kg/m^3
μ	Viscosity	1.0×10^{-2}	1.0×10^{-5}	$(N \cdot s)/m^2$
σ_0	Surface tension coefficient	0.072		N/m
d_0	Characteristic length	0.005	-	m

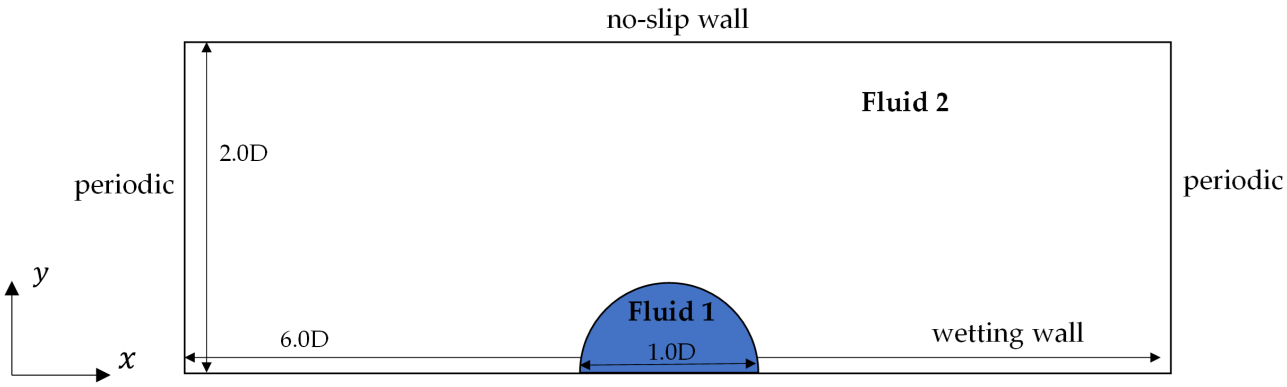

Fig. 1 Computational model (A)

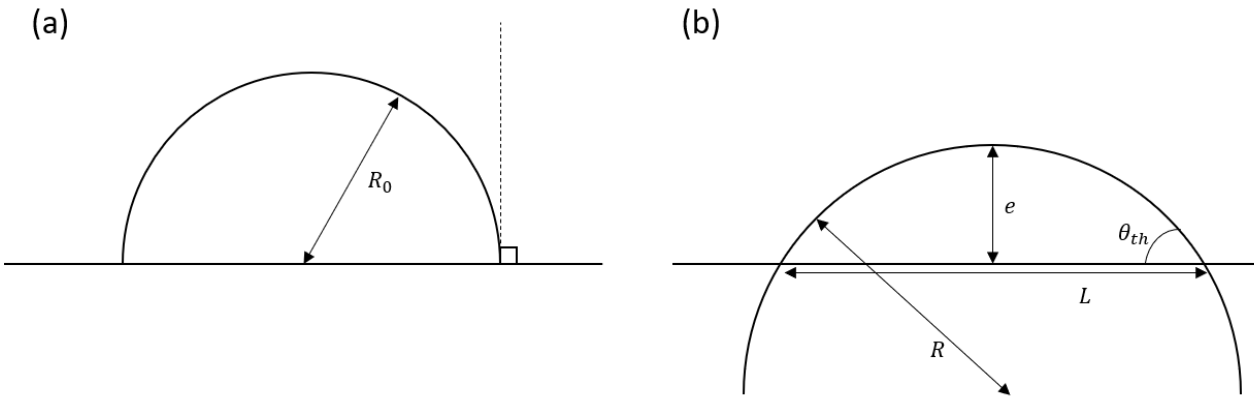

Fig. 2 (a) Definition of $\boldsymbol{R_0}$ on initial drop shape, (b) Definition of $\boldsymbol{R}$, $\boldsymbol{e}$, $\boldsymbol{L}$ on final drop shape

The calculation parameters in **Table 1** are the same as in the previous study [6] for comparison of the calculation results. The number of computational grids is set to 64 grids per 1.0D of characteristic length. The periodic boundary condition is applied to the sidewalls because it is an asymmetric phenomenon, and the no-slip condition is applied to the boundary condition of the velocity on the upper and lower walls.

Validation calculations are performed on this computational model by varying the set contact angle in Eq. (11) from 30° to 140° in 10° increments until the interface position becomes steady for each parameter. We validate the droplet final shape by comparing the horizontal length L on the wall and the maximum vertical length e from the wall with the analytical solution derived from mass conservation.

3.1.2 Results

Fig. 3 shows the results of this study for the final shape of the gas-liquid interface at each set contact angle.

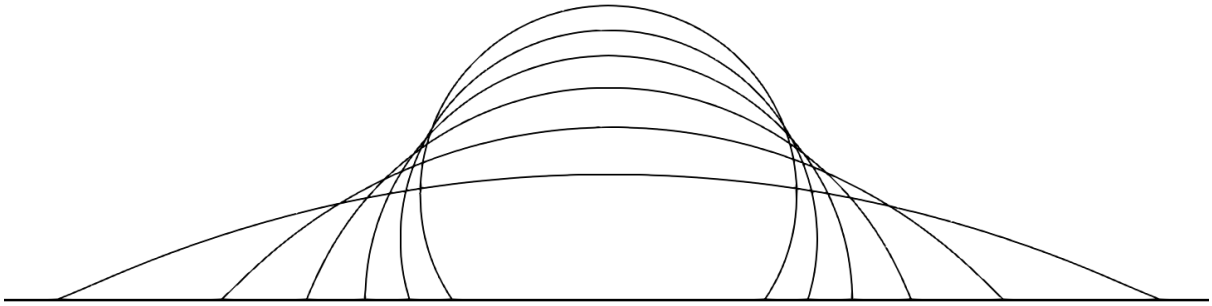

Fig. 3 Final drop shape on $\boldsymbol{\theta_{th}} = \mathbf{30°, 50°, 70°, 90°, 110°, 130°}$

The droplet radius R, the horizontal length L of the droplet on the wall, and the vertical maximum length e from the wall in the final shape can be given by equation (12) by considering the mass conservation law.[6)]

$$R = R_0\sqrt{\frac{\pi}{2(\theta_{th}-\sin\theta_{th}\cos\theta_{th})}}\ ,\quad L = 2R\sin\theta_{th}\ ,\quad e = R(1-\cos\theta_{th}) \tag{12}$$

The analytical solution expressed by Eq. (12) is plotted as solid and dotted lines, and the analytical result of this study is plotted as red and blue circles, as shown in **Fig. 4**.

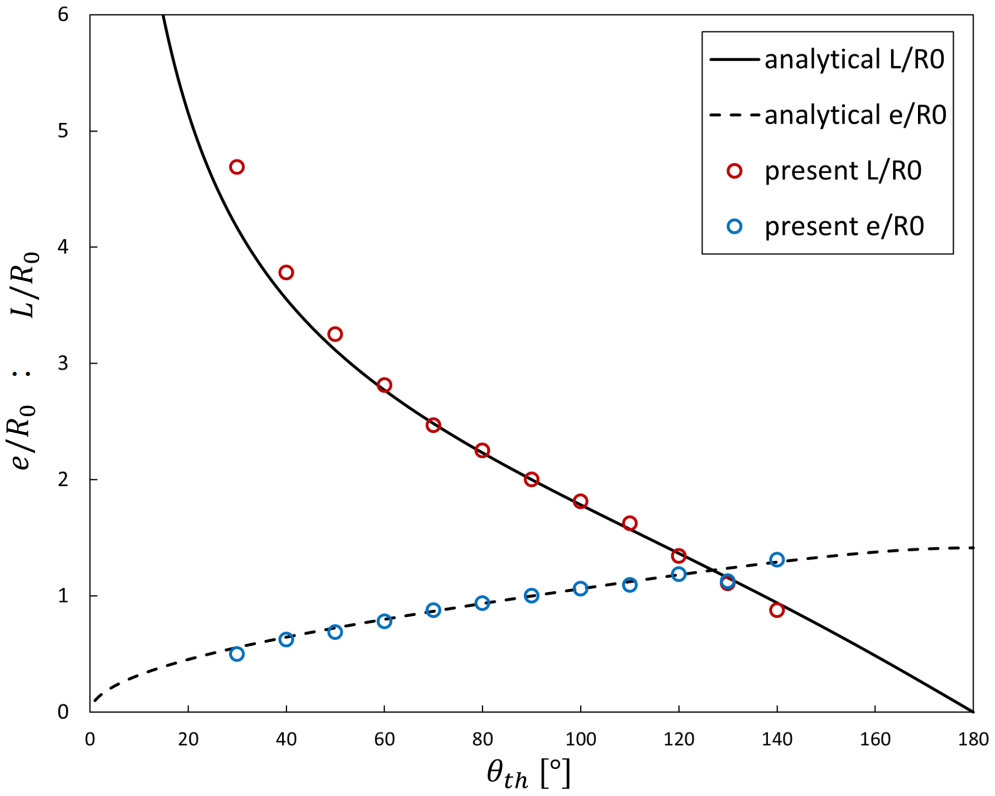

Fig. 4 Geometrical characteristic of the drop versus the contact angle $\boldsymbol{\theta_{th}}$

In the range of $60° \le \theta_{th} \le 120°$, the deviation from the analytical solution is at most 3% for both e/R_0 and L/R_0. Especially in the range of $70° \le \theta_{th} \le 100°$, the deviation is within 1%, which means that the interface shape is in good agreement. For $\theta_{th} = 30°, 40°, 130°$, and $140°$, the deviation from the analytical solution became larger as the contact angle moved away from 90°. Especially for $\theta_{th} = 30°$, the deviation became as large as 10%. These results indicate that our method is not sufficient to simulate the wettability in the small contact angle region.

3.2 (B) Droplet migration by temperature difference Marangoni convection

To validate the case of the simulated temperature variation of surface tension, we calculate the liquid-liquid two-phase flow in which droplets move due to temperature difference Marangoni convection. The validation is performed by comparing the calculation results with those of the previous study [7].

3.2.1 Computational model

The computational model used in this section is shown in **Fig. 5**. The physical properties of the working fluid used in the analysis are shown in **Table 2**.

Table 2 Physical parameters of the fluid

Symbol	Parameter	Fluid 1	Fluid 2	Unit
ρ	Density	250	500	kg/m^3
μ	Viscosity	0.012	0.024	$(N \cdot s)/m^2$
k	Thermal conductivity	1.2×10^{-6}	2.4×10^{-6}	$W/(m \cdot K)$
C_p	Isobaric specific heat capacity	5.0×10^{-5}	5.0×10^{-5}	$J/(kg \cdot K)$
σ_0	Surface tension coefficient	1.0×10^{-2}		N/m
σ_T	Temperature coefficient of surface tension	2.0×10^{-3}		$N/(m \cdot K)$
d_0	Characteristic length	1.44×10^{-3}	-	m
ΔT	Temperature difference per characteristic length	0.0288		K

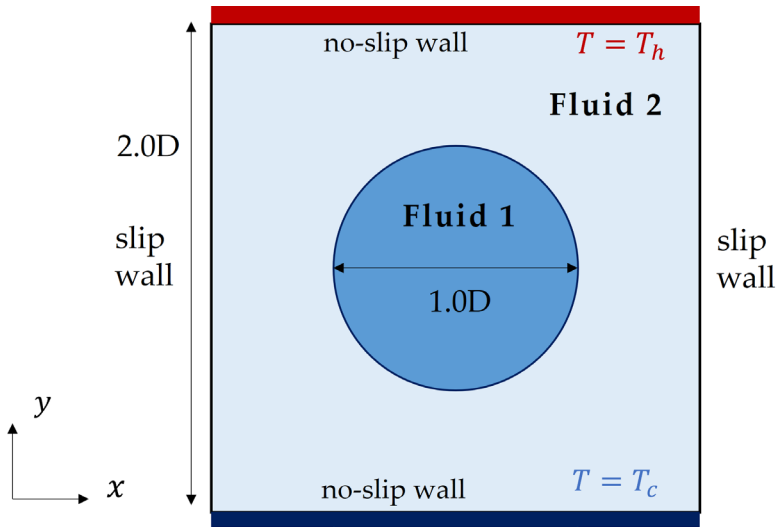

Fig. 5 Computation model (B)

The calculation parameters in **Table 2** are the same as in the previous study [7] for comparison of the calculation results. The number of computational grids is set to 64 grids per 1D of characteristic length.

In **Fig. 5**, T_h and T_c are set based on the temperature difference ΔT per characteristic length, and these values are given as the isothermal boundary conditions at the heating and cooling surfaces. The temperature difference on the interface causes Marangoni convection, and the droplet rises are calculated. Validation of the consideration of temperature variation in surface tension is performed by comparing the droplet rise rate with the results of the previous study [7].

3.2.2 Results

The visualization of the temperature field and velocity vector after sufficient time evolution is shown in **Fig. 6**, and the

comparison of the droplet rise velocity with previous study is shown in **Fig. 7**.

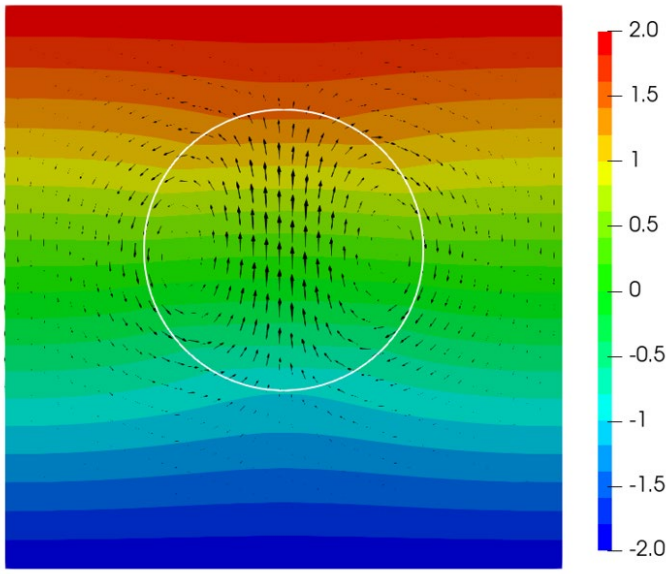

Fig. 6 Temperature field and velocity vector developed by Marangoni convection ($\boldsymbol{\tau = 2.0}$)

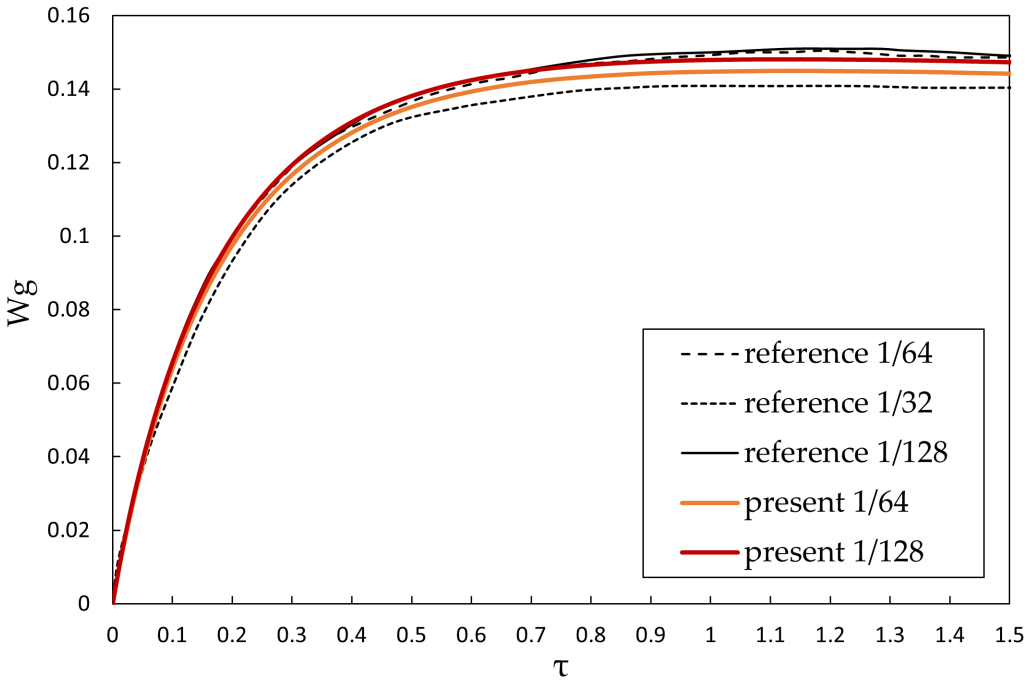

Fig. 7 The migration velocity of the drop versus time

Fig. 6 shows the development of an upward velocity field inside the droplet due to the Marangoni effect, indicating that the same Marangoni convection phenomenon as in the previous study can be reproduced.

Fig. 7 shows a comparison of the time response of the droplet rise rate. The transition of the time response is very similar to that of the graph when compared to the calculation results of previous study. The tendency of the time response graph of the ascending velocity to show micro-oscillation, which was observed when the same calculation was performed using the Level Set method, was not confirmed in this calculation.

The value of the terminal velocity at $\tau = 1.50$ differs by about 3% from the result of a previous study with a similar number of grids (reference 1/64), and this difference is reduced to within 1% when the number of grids is doubled (present 1/128). This result is in good agreement with the results of the previous study with the maximum number of grids (reference 1/128), which confirms the validity of considering the temperature dependence of the surface tension in the present method.

4. Conclusion

We focused on fluid phenomena in which surface tension is dominant, such as Marangoni convection and wetting phenomena, and investigated numerical methods for these phenomena. The Conservative Phase Field method, which has been attracting attention in recent years as a method to track the gas-liquid interface while maintaining the interface width without including the switching of treatment near the interface region., was introduced, and a method coupling the Level Set method was applied to capture the surface behavior accurately. The validity of the proposed method was verified using a benchmark problem, and the usefulness of the method for various surface tension-driven phenomena was examined. As a result, the following findings were obtained for the proposed method.

Validation (A): Simulation of wettability on a solid wall

- In the range where the contact angle was close to $90°$, the interface shape corresponding to the contact angle showed good agreement.
- In the range where the contact angle is smaller than $50°$ and larger than $110°$, the simulated wettability by the contact angle using this method is not sufficient, and further verification and improvement are needed.

Validation (B): Simulation of the temperature variation of surface tension (temperature-differential Marangoni convection)

- The present method successfully reproduced the Marangoni convection phenomenon in the benchmark problem.
- In the calculations with a larger number of grids, the results are in good quantitative agreement with previous study.
- The oscillations that were observed when the model was calculated using the Level Set method did not occur in this method, and the graphs had a similar shape as in the previous study.

References

1) P. Chiu and L. Yan-Ting : *J. of Comp. Physics* **230.1** (2011): 185-204.
2) D. Jeong and K. Junseok : *Computers & Fluids* **156** (2017): 239-246.
3) K. Yokoi : *J. of Comp. Physics* **278** (2014): 221-228.
4) L. Liu and L. Taehun : *Int. J. of Modern Physics* C **20.11** (2009): 1749-1768.
5) A. Fakhari and B. Diogo : *J. of Comp. Physics* **334** (2017): 620-638.
6) J. Dupont and L. Dominique : *J. of Comp. Physics* **229.7** (2010): 2453-2478.
7) I. Seric, A. Shahriar, and K. Lou : *J. of Comp. Physics* **352** (2018): 615-636.